Dynamic environment but no temperature change since the late Paleogene at Lühe Basin (Yunnan, China)

Caitlyn R. Witkowski[1,2], Vittoria Lauretano[1,2], Alex Farnsworth[3], Shu-Feng Li[4], Shi-Hu Li[5,6], Jan Peter Mayser[1,2], B. David A. Naafs[1,2], Robert A. Spicer[4,5], Tao Su[4], He Tang[4,8], Zhe-Kun Zhou[4], Paul J. Valdes[3], Richard D. Pancost[1,2]

[1]School of Earth Sciences, and Cabot Institute, University of Bristol, Bristol, BS8 1TS, UK
[2]Organic Geochemistry Unit, School of Chemistry, University of Bristol, Bristol, BS8 1QU, UK
[3]School of Geographical Sciences and Cabot Institute, University of Bristol, Bristol, BS8 1SS, UK
[4]CAS Key Laboratory of Tropical Forest Ecology, Xishuangbanna Tropical Botanical Garden, Chinese Academy of Sciences, Mengla 666303, China
[5]State Key Laboratory of Lithospheric Evolution, Institute of Geology and Geophysics, Chinese Academy of Sciences, Beijing 100029, China
[6]Lancaster Environment Centre, Lancaster University, Lancaster, LA1 4YQ, UK
[7]School of Environment, Earth and Ecosystem Sciences, The Open University, Walton Hall, Milton Keynes, MK7 6AA, UK
[8]State Key Laboratory of Isotope Geochemistry, Guangzhou Institute of Geochemistry, Chinese Academy of Sciences, Guangzhou 510640, China

Correspondence to: Caitlyn R. Witkowski (caitlyn.witkowski@bristol.ac.uk)

Supplemental Text

TOC (wt %) analyses

Total Organic Carbon (TOC) was determined on 56 samples using an Elementar vario PYRO cube at the University of Bristol, analysing C/N/S via catalytic combustion/reduction (1150 °C), optimised for coupling with an Isoprime IRMS for simultaneous determination of stable isotope ratios of C and N. Detection limits are at 0.001% or 10 ppm for C/N/S. An NC Soil reference standard was used to determine analytical precision. Prior to the analyses, all samples were prepared through an acid pre-treatment for carbonate removal, following the method by Hedges and Stern (1984).

Lipid extraction

For 56 samples from the Lühe coalmine section, 5 g of freeze-dried homogenised sediment were extracted using an Ethos Ex microwave extraction system with 20 ml of dichloromethane (DCM) and methanol (MeOH) (9:1 v/v). Microwave extractions were set using a 10-minute ramp to 70°C (1000W), a 10-minute hold at 70°C (1000W), and 20-minute cooling. Samples were then centrifuged at 1700 revolutions per minute (rpm) for 5 min to promote extract and sediment separation. Supernatants were removed and collected, and about 10 mL of DCM:MeOH (9:1 v/v) was added to the remaining sample and centrifuged again, before combining the available supernatants. This procedure was repeated up to five times to maximise lipid extraction. Elemental sulphur was removed by the addition of activated copper to the total lipid extract (TLE), left overnight. The TLE was concentrated by rota-evaporation and washed through a 4-cm sodium sulphate column using DCM:MeOH (9:1, v/v) to remove sediment particles. Subsequently, the TLE was split in two aliquots, and one of these was separated over a 4-cm alumina column by elution in an apolar fraction using hexane:DCM (9:1 v/v, 5 ml), and a polar fraction using DCM:MeOH (1:2 v/v, 4 ml). The apolar fraction was re-dissolved in hexane and analysed by GC-MS. The polar fraction was re-dissolved in hexane:isopropanol (99:1, v/v) and passed through a 0.45 μm polytetrafluoroethylene filter before analyses by HPLC-MS.

Gas chromatography-mass spectrometry

Apolar fractions were analysed at the University of Bristol using a Thermo Scientific ISQ Single Quadruple gas chromatography mass spectrometry (GC-MS) system, fitted with a fused HP-1 silica capillary column (50 m x 0.32 mm i.d., 0.17μm film diameter). Using helium as the carrier gas, 1 μL of sample dissolved in hexane was injected at 70℃ using an on-column PTV injector in splitless mode. The temperature program was set to four stages: 70℃ hold for 1 min, ramping to 130℃ at 20℃/min, then ramping to 300℃ at 4℃/min, and finally holding 300℃ for 20 min. The electron ionisation (EI) source was set at 70 eV. The emission current was set to 150 μA and scanning occurred between m/z ranges of 50-650 Daltons in full scan mode. The instrument accuracy was determined using an external fatty acid methyl ester (FAME)

standard. Compound identification was carried out based on published spectra, characteristic mass fragments, and retention times.

High performance liquid chromatography/atmospheric pressure chemical ionisation – mass spectrometry

Filtered polar fractions were analysed by high performance liquid chromatography/atmospheric pressure chemical ionisation – mass spectrometry (HPLC/APCI-MS), using a ThermoFisher Scientific Accela Quantum Access Triple quadrupole MS at the University of Bristol. Normal phase separation was achieved using two Waters Acquity UPLC BEH Hilic columns (2.1×150 mm; 1.7 μm i.d.) with a flow rate of 0.2 ml min^{-1}, following the method by Hopmans et al. (2016). Samples were eluted using a linear gradient of hexane hexane:IPA (9:1, v/v) (Hopmans et al., 2016), from an injection volume of 15 μL, out of 100 μL. Analyses were performed using selective ion monitoring mode (SIM) to increase sensitivity and reproducibility (m/z 1302, 1300, 1298, 1296, 1294, 1292, 1050, 1048, 1046, 1036, 1034, 1032, 1022, 1020, 1018, 744, and 653), and M + H+ (protonated molecular ion) GDGT peaks were manually integrated.

Additional GDGT calculations

The Branched vs. Isoprenoidal Tetraether (BIT) index was also calculated. Typically used to indicate the relative input of terrestrial and marine organic matter, here BIT was used to confirm that these sediments were not deposited in a deep lacustrine setting which could be indicated by isoprenoidal GDGTs. BIT is defined by (Hopmans et al., 2004) as:

BIT= (Ia+IIa+IIa'+IIIa+IIIa') / (Ia+IIa+IIa'+IIIa+IIIa'+ Crenarchaeol)

In addition to bacterial brGDGTs (Fig. S1), this includes the isoprenoidal (iso)GDGT known as crenarchaeaol, which is produced by Thaumarchaeota and is especially abundant in marine settings. The BIT values of 1.0 throughout the section indeed confirm our assumptions (data in Table S1).

Supplement references

Hedges, J.I., Stern, J.H.: Carbon and Nitrogen Determinations of Carbonate-Containing Solids, Limnology and Oceanography, 29, 657-663, 1984.

Hopmans, E.C., Schouten, S., Sinninghe Damsté, J.S.: The effect of improved chromatography on GDGT-based palaeoproxies, Organic Geochemistry, 93, 1–6. https://doi.org/10.1016/j.orggeochem.2015.12.006, 2016.

Hopmans, E.C., Weijers, J.W.H.H., Schefuß, E., Herfort, L., Sinninghe Damsté, J.S., Schouten, S.: A novel proxy for terrestrial organic matter in sediments based on branched and isoprenoid tetraether lipids, Earth and Planetary Science Letters 224, 107–116. https://doi.org/10.1016/j.epsl.2004.05.012, 2004.

Table S1. All biomarker data for climatic and environmental change at Lühe basin. All numerical data derived from biomarkers are included in this table. The grey columns include sample information, including the section name, sample code, depth from base (m), and lithology recorded from the original log. The lavender columns include bulk information, including average organic carbon percentage (OC%), total nitrogen percentage (TN%), carbon to nitrogen ratios (C/N ratio), and the stable carbon isotopic composition of the bulk carbon ($\delta^{13}C$ (VPDB)). The yellow columns include branched GDGT results for the methylation of branched tetraethers based on the temperature-dependence of 5-methyl brGDGT (MBT'5me), the branched-to-isoprenoidal (BIT) GDGT index, the CBT, and pH based on CBT. The green column includes the three different brGDGT-based temperatures based on calibrations tuned to peat, soil, or lake environments. The blue columns include the indices derived from the apolar fractions (i.e., hopane and n-alkane), including indices for interpreting the thermal maturity (carbon preference index (CPI) and the ββ/(αβ+βα+ββ stereochemistry of C29 and C31 hopanes) and n-alkane-based indices for interpreting the depositional environment (average chain length (ACL), P-aqueous ratio (Paq), and C23/(C23+C31) n-alkane ratio). See accompanying spreadsheet.

Table S2. Terpenoid data for vegetation change at Lühe basin. The grey columns include sample information, including the section name, sample code, depth from base (m), and lithology recorded from the original log. The green columns track seven diterpenoids (i.e., cadalene, norpimerane, 19-norabietane, 19-Norabieta-8,11,13-triene, dehydroabietane, 10,18-bisnorabieta-5,7,9(10),11,13-pentaene, simonellite) and the pink columns track two triterpenoids (i.e., tetramethyl-octahydrochrysene and des-A-lupane) throughout the whole section. Each terpenoid is labelled along with its molecular weight (MW), diagnostic fragments (mass-to-charge ratio, m/z), and retention time in the analytical runs. The "x" symbol and colour shade indicate the relative abundance of each biomarker in the analytical runs of the apolar fractions, relative to the other compounds in each run, where [no x / white] = absent, [x / light] = trace amounts, [xx / mid colour] = present, and [xxx / dark colour] = highly abundant. On the side of the table, Fig. S3 and S4 have been included for reference to the individual compound structures. See accompanying spreadsheet.

Table S3. Environmental interpretation of Lühe basin. Overall, the Lühe coalmine section represents various depositional environments typically found in a floodplain setting: active and abandoned channel deposits, proximal to distal overbank crevasse splay deposits, sub-aerial soils to shallow ponds swamps and, rarely, deeper lakes. The only possible candidate for a deep lake setting in the mine section is the part of the succession between 216 and 224 m. Most of the sands have a tuffaceous component and ash beds are preserved in the pond/swamp settings. In the mine there is no clear evidence of the deep long-lived lake seen in the Lühe Town section. The fluvial sediments that predominate from 85-200m contain large log 'jams' and detrital zircons, the youngest of which are dated to ca. 33 Ma (Wissink et al., 2016). See accompanying detailed log (Fig. S5).

Depth from base (m)	Environmental interpretation
0-2.5	Siliciclastic-rich 'coal' suggesting a swamp, possibly with open water, in which accumulated both organic remains and muds.
2.5-3.5	Grey clay suggesting a more open water pond, or temporary flooding from a channel located some distance from the depositional site, with less organic input.
3.5-7.1	Coarsening upward silt to fine sand indicative of a sudden influx of sediment during flood conditions. Possibly overbank crevasse onto the interfluve. Flood conditions brought in river transported wood fragments.
7.1 - 11.75	Return to pond/swamp conditions on the interfluve, and high organic input, but this unit is disturbed by modern day slumping.
11.75-17.5	More active silt influx to the pond (perhaps the channel migrating closer, or a small stream starts flowing into the pond bringing in rafted branches and leaves, and eventually silting up the pond). As it shallows the surface becomes colonised by aquatic or terrestrial plants indicated by rooting, and subaerially exposed and oxidized (reddish colour).
17.5-20	Return to open, but organic-rich pond/swamp conditions as compaction/extension and basin floor drop provides more accommodation space.
20-20.75	Another small influx of fine sand - possibly distal crevasse splay, bringing in transported leaves.
20.75-28	Return to swamp conditions. Not a pure peat so suggesting occasional ingress of fine siliciclastic (clays and silts) by periodic rises in the water table and slow lateral water movement.
28-40.1	Gradual increase in water flow bringing in ever coarser siliciclastics. This fills up the swamp and provides stable subaerial or near sub-aerial surfaces long enough for some plant colonization (rooting). Occasional quiet water phases as water table fluctuates, but the overall trend is coarsening upwards indicative of a lateral approach of a river channel. This gives rise to more frequent flood inundations, bringing in fragmented leaves and some more coherent sand bodies.
40.1-47.9	Very shallow pond transforming, briefly, to sub-aerial conditions at around 44 m, with the surface colonised by plants, before the water slightly deepens again.
47.9-49	Sudden influx of sand by fluvial activity, giving rise to crossbedding suggesting migration of sand body into and across the pond sediment surface.
49-53	After a temporary return to shallow pond conditions before another influx of sand in a crevasse splay event bringing in leaf material, fining upwards to a near sub-aerial stable surface colonised by plants.
53-62.2	Continued subsidence leads to a return to an organic-rich swamp. This was not just a sphagnum peat but a swamp that existed long enough to develop a standing forest. During this time several eruptions deposited ash horizons, not admixed with other siliciclastics, so showing no lateral water movement. One of these, the one preserving a standing tree stump, is dated as ca. 33 Ma. Some Fe+++ concretions confirm anoxic conditions.
62.2-64.5	Distal crevasse splays invade the swamp and in-washing branches.
64.5-69	Shallow pond on the interfluve floodplain, eventually colonised by plants.
69-76.9	Gradual increase in the energy of influx of sediment, distal from a channel, colonised by plants. At 74.2 m a major sand incursion like that at 47.9-49m occurred, bringing in branches/logs.

	Crossbedding suggests lateral sand migration in a channel, although there is no evidence of basal erosion so if it likely to have been the result of a flood event. Evidently the main channel is getting closer.
76.9-85.8	More overbank flood deposits not too far from a main channel. Flood events infrequent enough to allow establishment of vegetation to begin, but this was followed by a rapid influx of silts before less frequent inundations returned. A small short-lived pond developed before more silt arrived and plants recolonised.
85.8-97.9	High energy overbank incursion that must have eroded some of the pre-existing silts, but no evidence of deep erosion (e.g., large scours), but medium to coarse sand fining upwards suggest the influence of a major channel. Periodic sand influxes repeat, with main channel activity evidenced by the ca. 8 m-thick cross-bedded sand body washing in leaf debris. There is evidence of a reversal of flow direction, possibly suggesting a laterally migrating channel.
97-9-101.3	Channel flow migrates elsewhere on the floodplain leaving a shallow pond that infrequently receives flood silts and becomes colonised by plants.
101.3-105.5	Channel sand again, with large scale crossbedding indicating consistent flow direction, interspersed with quiescent episodes of shallow water where ripples develop. This suggests highly variable flow in the channel. This sand is topped by an erosional surface and a transition to silt deposition.
105.5-117.5	Silts indicative of 1) overbank deposition or 2) accumulation in an abandoned channel. 1) is more likely because the silts are immediately colonised by plants, which then stops, suggesting more active/frequent inundation at time goes on. If 2) then the opposite pattern would be expected.
117.5-132.1	Channel activity returns, but this time the sand is a lighter colour suggesting a possible change of source or a greater mix of volcanics. The basal sand is cross-bedded in the opposite direction to the sands at 101.3-105.5 and contains in-washed plant debris. The flow slackens and this is the start of a succession of silty fine sands, some of which are rooted and cross-bedded that inundate the floodplain, derived from the nearby main river channels. These overbank deposits also incorporate plant debris and between flood events subsidence leads to the formation of organic-rich ponds or short-lived swamps.
132.1-135	A more quiescent period with less energetic inundation.
135-142.8	Return of major channel influence with cross-bedded fine to medium sand and a return to the same composition as dominated in the basal part of the section, and dominance of the same flow direction. This probably represents sand inundation of the floodplain incorporating plant debris as there is no strong basal scour and the unit quickly fines up near the top. This suggests a one-time event.
142.8-146.8	Return to a swamp, with one silt inundation event before swamp conditions persist for some time. Anoxic enough (either deep or with a very high organic input exceeding oxidation) for Fe++ mobilisation, now represented as concretionary iron horizons.
146.8-158.1	More river influence, flood inundations, at first distal and remaining stable for long enough to be plant colonised, becoming more proximal and with higher deposition rates at ca. 150 m before receding again and the sediments, bearing in-washed logs, becoming plant colonised. Short-lived swamp and possibly sub-aerially exposed floodplain silts colonised by plants cap this interval.
158.1-162.8	A sudden increase in iron-stained medium sand, cross-bedded near the top, suggests more inundation of the flood plain by overbank activity. There is no evidence of an erosional base suggesting this was not a major channel, but overbank discharge. This could have been a single event that incorporated plant debris, but there was no time for rooting to develop. This is capped by a local erosional surface.
162.8-163.4	Here fluvial activity is truncated at least twice by high energy erosion events.
163.4-200.8	This interval represents major river channel influences. It comprises at least seven episodes of channel activity and one significant local erosion event. The succession begins with a single overbank depositional even after which the deposit remained stable long enough for vegetation to

	colonize it and some incipient soil processes to begin. There is then a depositional hiatus before a major deposition of fine cross-bedded sand showing unidirectional flow occurred. At 183.5 m deposition briefly became more quiescent with a shallow pond developing before sand deposition resumed. At 187 m a brief pulse of increased flow washed in logs. Steady sand deposition with unidirectional flow and transported plant debris returned. This succession was truncated at 197.4 m by an erosional surface, but the sand deposition then continued as before, suggesting perhaps this erosional event was short-lived and did not change substantially the nature of the depositional package.
200.8-207.6	The episode of sand deposition ceases with the development of a long-lived pond floodplain environment in which muds accumulated, eventually to be colonised by plants. At ca. 204 m a white clay that could be an altered ash deposited either in a shallow pond or sub-aerially, briefly interrupts the succession, which returns to mud deposition with an episode of swamp conditions before a local erosion event truncates the unit.
207.6-209.8	A series of erosive high energy fluvial inundations of the floodplain indicate a proximal channel, but its influence is short-lived and ends with a crevasse splay sand incorporating plant debris.
209.8-215.9	This represents a return to shallow pond deposition with the pond eventually silting up and the surface being colonised by vegetation. Compaction/tectonic lowering of the surface leads to it drowning and the return of swamp conditions.
215.9-233.3	There appears to be a local drop in base level at this point because swamp to lake to swamp conditions dominate for some while. This begins with what appears to be the formation of a swamp occupied by vegetation rooted in the underlying muds, or deep-water anoxic and highly organic conditions formed suddenly, so drowning the mud-rooted vegetation. This lake/swamp organic accumulation was interrupted only by a succession of four minor ash falls. After the last of these at 224 m the lake had evidently filled with organics and a near subaerial surface had developed occupied by trees as evidenced by both fallen logs and tree stumps preserved in life position. This swamp was eventually flooded to form an open pond environment and as the shoreline receded from this location (the lake increased in surface area but remained shallow enough for plants to grow) organic input decreased leading to a predominance of rooted clay deposition. This succession was terminated by an erosional surface.
233.3-250	Fluvial influence returns with what appears to be a crevasse splay with an erosional base. Cross bedding suggests progressive migration of the sand body into and across the shallow pond, followed by a more powerful channel influence with large-scale crossbedding. River transported plant fragments occur throughout. There is a brief influx of coarser material with an erosional base at 239.5-240.1 m and evidently flow and winnowing increased for a short time, followed by a return to fine sand deposition, before the energy of the system waned further leading to a short-lived return to pond or floodplain deposition. Rooting suggests at most very shallow water depths. This system is then inundated by another sand body, at the top of which there is evidence of a waning and then temporary cessation of deposition leading to an increasing concentration of plant debris and the surface becoming colonized by vegetation, including trees.
250-271.5	This interval represents a period of floodplain deposition in which shallow pond/swamp environments predominate, interrupted only briefly by sand inundations during minor flooding events. Most of the sediments host tree stumps in life position and/or fallen logs and abundant rooting. Water depth, if any, is shallow and soil forming conditions predominate. Identifiable plant remains are rare, presumably to due to oxidation and the activity of detritivores. There may be pond formation at ca. 266 m but that quickly silts up again by 270 m.
271.5-300.5	This interval represents a return to strong frequent fluvial deposition, interspersed with shallow pond formation during more quiescent intervals. The succession starts with periodic thin incursions of fine sand which then become thicker and retain crossbedding. There are at least six of these major sand incursions separated by shallow pond deposition. Lenticular bedding may just mean we are looking long the flow axis. The large amounts of iron suggest erosion and oxidation

	of iron chelated onto organics in the drainage. There is not much evidence of rooting, which suggests this whole package was deposited relatively quickly, before vegetation had change to establish itself on the fluvial sediments, even during quieter times between depositional episodes.
300.5-316.8	This marks a reversion to swamp/pond/floodplain interfluve conditions. A swamp developed on the silts capping the fluvial sands and this lasted long enough to support a swamp forest as evidenced by the stumps in life position and fallen logs. At 305 m there begins a period of more frequent minor mud and fine sand influxes into the swamp each event separated by time long enough for vegetation to establish itself on the sediment surfaces, before returning to a wooded swamp environment at 312.8 m. Minor mud/sand incursions begin again at 315.1m.
316.8-328.2	The rooted mudstones representing interfluve pond/ subaerial environments are truncated by a laterally migrating river channel that erodes into them. This cross-bedded lenticular sand body fines upward as the channel is abandoned and backfills with silt and becomes vegetated, despite minor sand incursions as at 323.4-324.1 m.
328.2-331	This represents another erosional small channel migration backfilled with mud.
331-340	This channel migration, infilling, development of vegetation, incursions by crevasse splays continues to the top of the section at 340m. The landscape is heavily forested as logs are common in the interfluve sediments and these are also rooted. Larger logs and other plant debris were transported by the channels as at 334-336m.

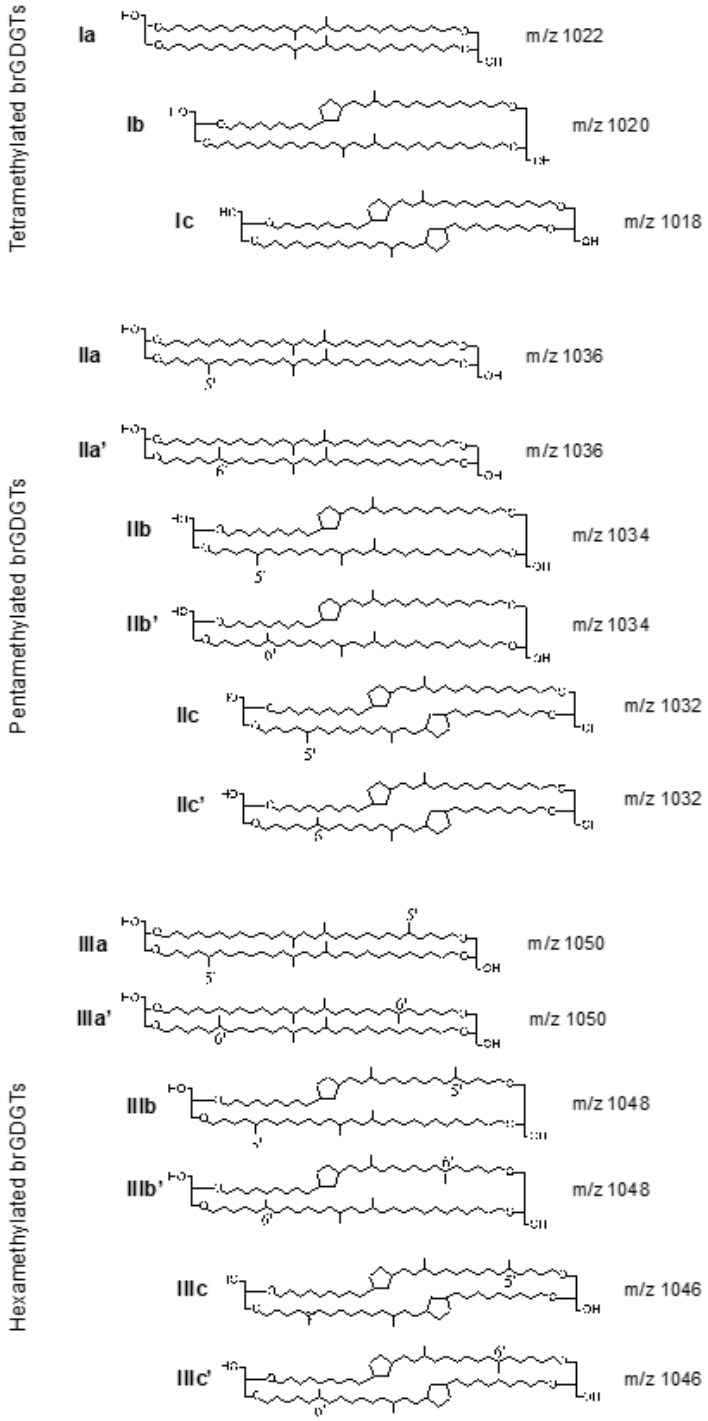

Figure S1. Structures of brGDGTs from this study.

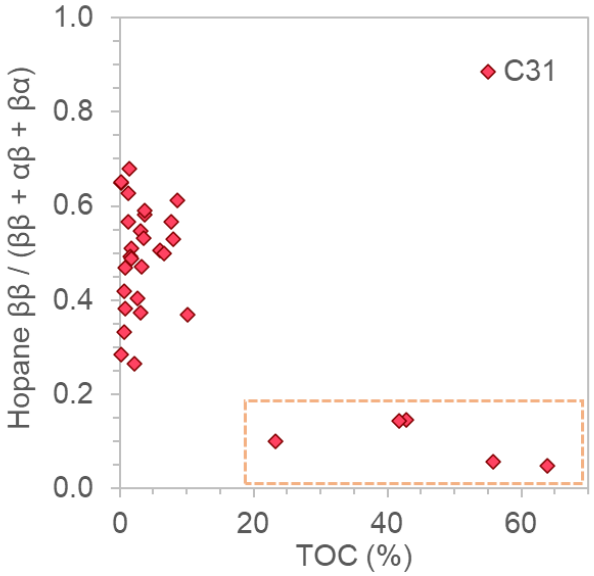

Figure S2. Hopane isomerisation ratio and total organic carbon (TOC%). High TOC% show very low hopane ratios, indicative of peatlands.

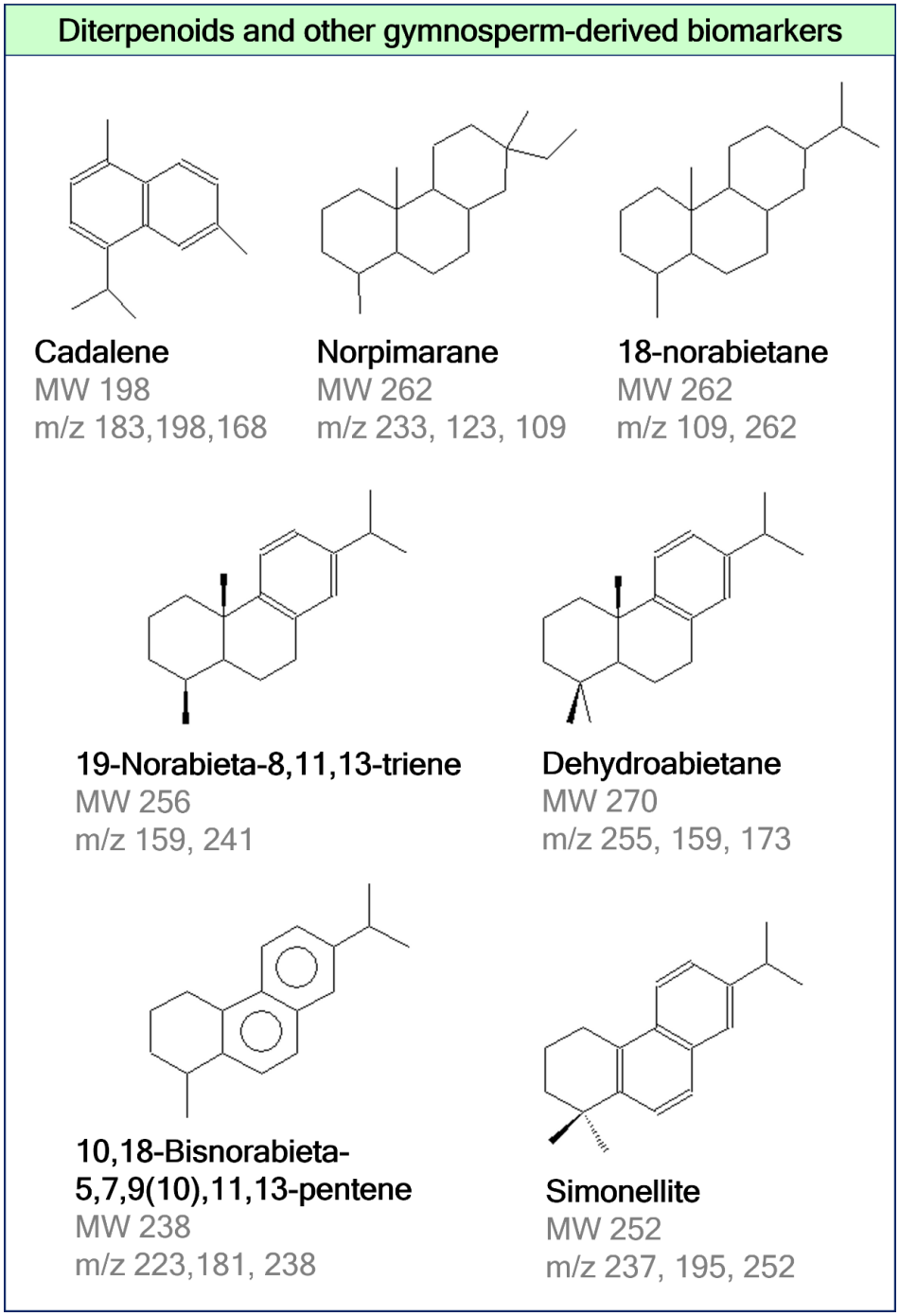

Figure S3. Biomarkers associated with gymnosperms found at Lühe Basin, in order of retention time. See corresponding Table S2 for presence and abundance of these biomarkers at each sample depth.

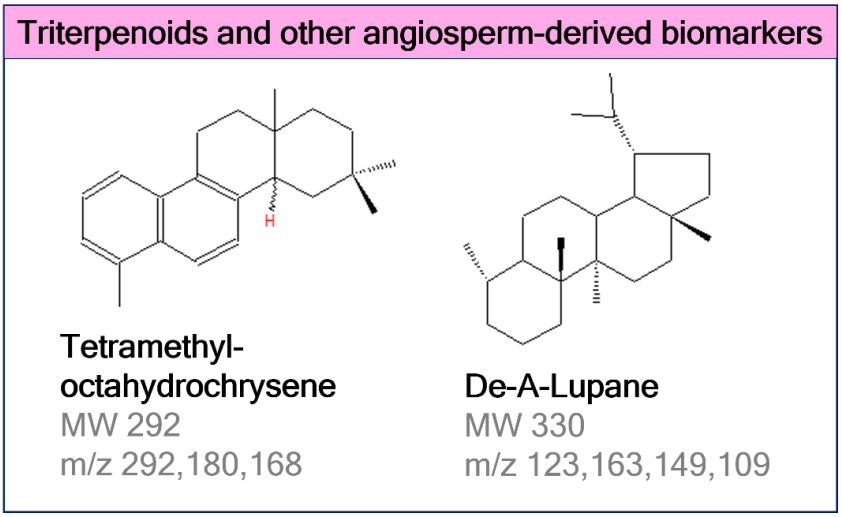

Figure S4. Biomarkers associated with angiosperms found at Lühe Basin, in order of retention time. See corresponding Table S2 for presence and abundance of these biomarkers at each sample depth.

Figure S5. Detailed sediment log at Lühe Basin. See accompanying figure.